UC Berkeley
UC Berkeley Previously Published Works

Title
Seismic soil-structure interaction in buildings. I: Analytical aspects

Permalink
https://escholarship.org/uc/item/9t09660m

Journal
J. Geotech. & Geoenv. Engrg., 125(1)

Authors
Stewart, Jonathan P
Fenves, Gregory L
Seed, Raymond B

Publication Date
1999

Peer reviewed

SEISMIC SOIL-STRUCTURE INTERACTION IN BUILDINGS. I: ANALYTICAL METHODS

By Jonathan P. Stewart,[1] Gregory L. Fenves,[2] and Raymond B. Seed,[3] Members, ASCE

ABSTRACT: Recent improvements in seismological source modeling, analysis of travel path effects, and characterization of local site effects on strong shaking have led to significant advances in both code-based and more advanced procedures for evaluating seismic demand for structural design. A missing link, however, has been an improved and empirically verified treatment of soil-structure interaction (SSI) effects on both the strong motions transmitted to structures and the structural response to these motions. This paper describes analysis procedures and system identification techniques for evaluating inertial SSI effects on seismic structural response. The analysis procedures are similar to provisions in some building codes but incorporate more rationally the influence of site conditions and the foundation embedment, flexibility, and shape on foundation impedance. Implementation of analysis procedures and system identification techniques is illustrated using a building shaken during the 1994 Northridge earthquake. The analysis procedures predict the observed SSI effects accurately. A companion paper applies these analyses to empirically evaluate SSI effects using available strong motion data from a broad range of sites and then develops general conclusions regarding SSI effects on seismic structural excitation and response.

INTRODUCTION

The seismic excitation experienced by structures is a function of the earthquake source, travel path effects, local site effects, and soil-structure interaction (SSI) effects. The result of the first three of these factors is a ''free-field'' ground motion. Structural response to free-field motion is influenced by SSI. In particular, accelerations within structures are affected by the flexibility of foundation support and variations between foundation and free-field motions. Consequently, an accurate assessment of inertial forces and displacements in structures can require a rational treatment of SSI effects.

Recent major advances have been made in state-of-practice procedures for characterizing earthquake source, travel path, and local site effects, as reflected in recent updates to code provisions by the Building Seismic Safety Council [BSSC (1997)] and International Conference of Building Officials (*Uniform* 1997). These advances have emerged largely as a result of strong motion data that has become available following recent earthquakes. For example, recent advances in the treatment of site effects were motivated by the significant ground motion amplification observed at soft, cohesive soil sites in major earthquakes such as the 1985 Mexico City and 1989 Loma Prieta events (Seed et al. 1988, 1992).

The state-of-practice for engineering characterization of SSI effects for ordinary structures has not undergone recent similar advancement, despite the availability of (1) a significantly broadened database of both free-field and structural strong motion recordings from recent earthquakes; and (2) sophisticated SSI analysis procedures. SSI analysis procedures include direct approaches in which the soil and structure are modeled together and analyzed in a single step and substructure approaches where the analysis is broken down into several steps. Simplified substructure-based SSI provisions are included in the BSSC (1997) and Applied Technology Council [ATC (1978)] codes, but these provisions have not been calibrated against a large inventory of field performance data as has been done for site effects.

The objectives of this paper and a companion paper (Stewart et al. 1999) are to make use of earthquake strong motion data to evaluate the effects of SSI on structural response for a range of site and structural conditions and then to use these results to calibrate simplified analytical procedures similar to those in the BSSC and ATC codes. This paper summarizes procedures for predicting SSI effects and reviews system identification procedures for evaluating SSI effects from strong motion recordings. In the companion paper, these procedures are applied for 57 sites in California and Taiwan with strong motion recordings to elucidate the effects of inertial SSI on seismic structural response and to verify the simplified analytical procedures.

SSI ANALYSIS PROCEDURES FOR DESIGN

Overview

Two mechanisms of interaction take place between the structure, foundation, and soil:

- *Inertial Interaction:* Inertia developed in the structure due to its own vibrations gives rise to base shear and moment, which in turn cause displacements of the foundation relative to the free-field. Frequency dependent foundation impedance functions describe the flexibility of the foundation support as well as the damping associated with foundation-soil interaction.
- *Kinematic Interaction:* The presence of stiff foundation elements on or in soil cause foundation motions to deviate from free-field motions as a result of ground motion incoherence, wave inclination, or foundation embedment. Kinematic effects are described by a frequency dependent transfer function relating the free-field motion to the motion that would occur on the base slab if the slab and structure were massless.

The focus of this paper is on inertial interaction, which can be the more important effect for foundations without large, rigid base slabs or deep embedment.

A system commonly employed for simplified analysis of inertial interaction, shown in Fig. 1, consists of a single-degree-of-freedom structure of height h on a flexible foundation medium represented by the frequency dependent and complex-valued translational and rotational springs $\bar{k}_u$ and $\bar{k}_\theta$. This sim-

[1]Asst. Prof., Dept. of Civ. and Envir. Engrg., Univ. of California, Los Angeles, CA 90095.

[2]Prof., Dept. of Civ. and Envir. Engrg., Univ. of California, Berkeley, CA 94720.

[3]Prof., Dept. of Civ. and Envir. Engrg., Univ. of California, Berkeley, CA 94720.
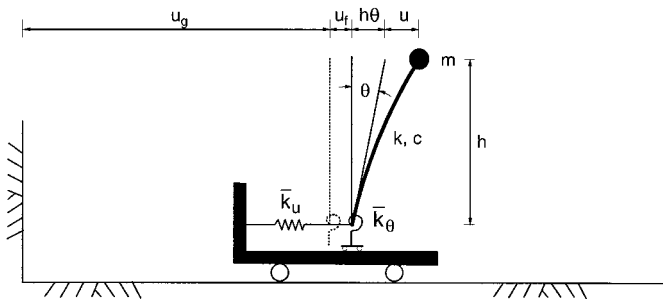
FIG. 1. Simplified Model for Analysis of Inertial Interaction

ple system can be viewed as a model of a single-story building or, more generally, as an approximate model of a multistory building that is dominated by the fundamental mode response. In the latter case, h is interpreted as the distance from the base to the centroid of the inertial forces associated with the fundamental mode.

Impedance Function

The impedance function is represented in Fig. 1 by $\bar{k}_u$ and $\bar{k}_\theta$ and may also include a coupling spring. Simplified impedance function solutions are available for rigid circular disk foundations located on the ground surface or embedded into a uniform, viscoelastic half-space. Terms in the impedance function are expressed in the form

$$\bar{k}_j = k_j(a_0, \nu) + i\omega c_j(a_0, \nu) \qquad (1)$$

where j denotes either deformation mode u or θ; ω = angular frequency (rad/s); a_0 = dimensionless frequency defined by $a_0 = \omega r/V_S$; r = foundation radius; V_S = soil shear-wave velocity; and ν = soil Poisson ratio. Foundation radii are computed separately for translational and rotational deformation modes to match the area A_f and moment of inertia I_f of the actual foundation (i.e., $r_u = \sqrt{A_f/\pi}$, $r_\theta = \sqrt[4]{4I_f/\pi}$). There are corresponding $(a_0)_u$ and $(a_0)_\theta$ values as well.

The real stiffness and damping of the translational and rotational springs and dashpots are expressed, respectively, by

$$k_u = \alpha_u K_u; \quad c_u = \beta_u \frac{K_u r_u}{V_S} \qquad (2a)$$

$$k_\theta = \alpha_\theta K_\theta; \quad c_\theta = \beta_\theta \frac{K_\theta r_\theta}{V_S} \qquad (2b)$$

where α_u, β_u, α_θ, and β_θ express the frequency dependence of the impedance terms; and K_u and K_θ = static stiffness of a disk on a half-space

$$K_u = \frac{8}{2 - \nu} Gr_u; \quad K_\theta = \frac{8}{3(1 - \nu)} Gr_\theta^3 \qquad (3)$$

where G = soil dynamic shear modulus.

Analytical procedures are available for the computation of impedance functions for rigid foundations, many of which are summarized in Luco (1980) and Roesset (1980). Adopted here is a widely used solution for a rigid circular foundation on the surface of a viscoelastic half-space (Veletsos and Wei 1971; Veletsos and Verbic 1973). However, the potentially significant effects of nonuniform soil profiles, embedded foundations, noncircular foundation shapes, flexible foundations, and piles or piers beneath the base slab must be taken into account. The following briefly discusses the effects of these factors on impedance functions.

Nonuniform Soil Profiles

The effective properties of profiles having a gradual increase in stiffness with depth can often be approximately modeled by an equivalent half-space, provided that the soil properties used to define the half-space shear-wave velocity V_S and hysteretic damping ratio β are judiciously selected. Roesset (1980) used soil properties from a depth of $0.5 \cdot r$ for this purpose. An alternative measure of effective profile velocity is obtained by computing the ratio of the profile depth to the shear strain-dependent shear-wave travel time through the profile. This approach was adopted for calculations of effective profile velocity in this study, using a profile depth of one foundation radius. The strain dependence of V_S and β can be estimated with site response analyses employing equivalent linear characterization of dynamic soil properties [e.g., Schnabel et al. (1972)]. Using these results, effective profile damping is estimated using a weighting function that decreases linearly from a maximum at the surface to zero at the profile depth. The foundation impedance of a finite soil layer overlying a rigid base is discussed by Kausel (1974) and Roesset (1980), although such profiles are seldom encountered in practice.

Embedded Foundations

The impedance of embedded foundations can be modeled in two ways: (1) Couple the increased static stiffness of embedded foundations with frequency dependent terms α_u, β_u, α_θ, β_θ for surface foundations [e.g., Elsabee and Morray (1977)]; or (2) use relatively rigorous analytical solutions for the impedance of a rigid foundation embedded into a half-space that account for dynamic basement wall/soil interaction effects [e.g., Bielak (1975) and Apsel and Luco (1987)]. The static stiffnesses of shallowly embedded foundations ($e/r < 1$) in a half-space can be approximated as follows:

$$(K_U)_E = K_U \left(1 + \frac{2}{3}\frac{e}{r}\right); \quad (K_\theta)_E = K_\theta \left(1 + 2\frac{e}{r}\right) \qquad (4)$$

Coupling impedance terms are small relative to $(K_u)_E$ and $(K_\theta)_E$ for small embedment ratios (i.e., foundation embedment/radius, $e/r < 0.5$). The BSSC (1997) code recommends use of (4) for embedded foundations.

The frequency-dependent α and β terms computed by Methods 1 and 2 for a cylindrical foundation embedded in a viscoelastic half-space ($\beta = 1\%$, $\nu = 0.25$) are compared in Fig. 2. For Method 1, stiffness terms α_u^* and α_θ^* are computed as the product of α_u and α_θ for surface foundations (Veletsos and Verbic 1973) and the depth effect modifiers on the right-hand sides of (4). Damping factors β_u^* and β_θ^* were similarly increased to reflect the higher static stiffness of embedded foundations. Stiffness terms α_u and α_θ from Methods 1 and 2 are comparable for $e/r < 0.5$, and in the case of α_θ, for $a_0 < 1.5$ as well. In the case of damping, the comparison in Fig. 2 is essentially one of radiation damping due to the low hysteretic soil damping in this example. Method 1 significantly under-predicts radiation damping for embedded foundations. However, these errors may be tolerable for low frequency structures ($a_0 < 1$) founded in soil with high hysteretic damping, as the radiation damping contribution to overall foundation damping can be relatively small in such cases.

To investigate the importance of embedment on SSI, the impedance of embedded foundations is evaluated in the companion paper using Method 1 and an adaptation of Method 2. The more rigorous Method 2-type analyses are based on the formulation by Bielak (1975) and more rigorously incorporate dynamic soil/basement-wall interaction effects into the foundation impedance function.

Foundation Shape

Impedance functions for foundations of arbitrary shape are commonly analyzed as equivalent circular mats, provided that the foundation aspect ratio in plan is <4:1 (Roesset 1980). An
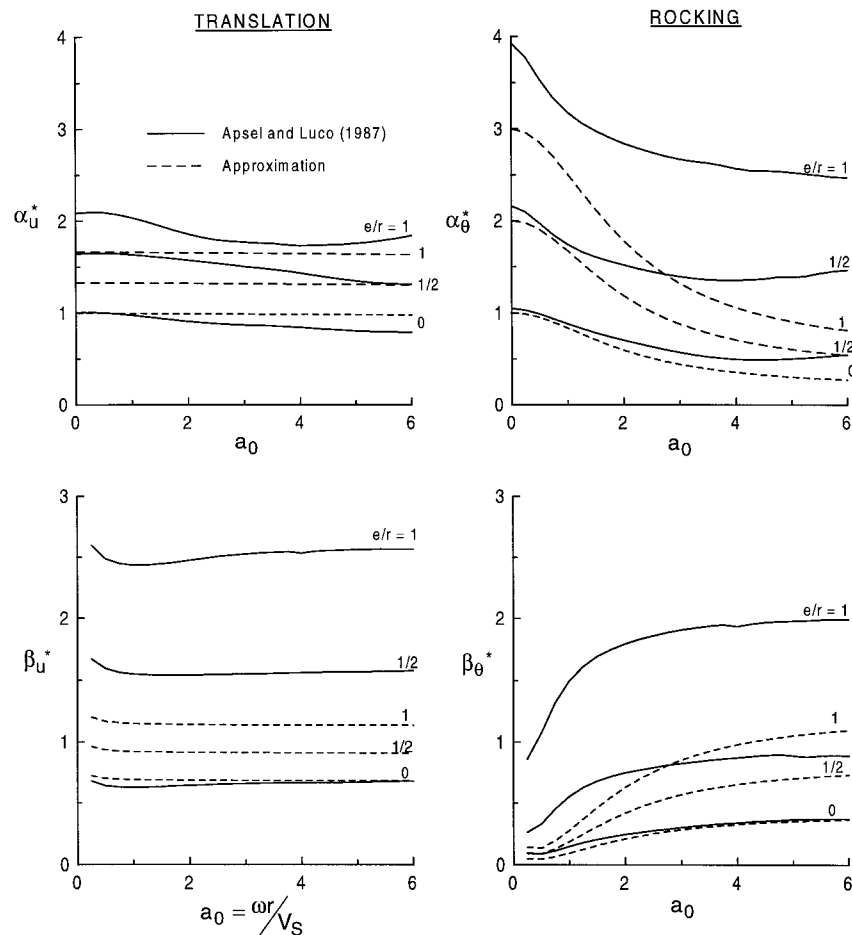
FIG. 2. Foundation Stiffness and Damping Factors for Rigid Cylindrical Foundations Embedded in Half-Space; Approximation versus Solution by Apsel and Luco (1987) [Asterisk (*) Denotes Modification to Parameters for Surface Foundations Taking into Account Effects of Embedment]

equivalent radius for translational stiffness is derived by equating the area of the mats, while an equivalent radius for rocking stiffness is derived by equating the moment of inertia of the mats. These criteria have been adopted into the BSSC (1997) code. Combining a number of analytical impedance function solutions from the literature for foundations of arbitrary shape, Dobry and Gazetas (1986) found that the use of equivalent circular mats is acceptable for aspect ratios < 4:1, with the notable exception of dashpot coefficients in the rocking mode. The radiation damping component of rocking dashpot coefficients was found to be underestimated by the equivalent disk assumption at low frequencies. Hence, radiation dashpot coefficients for oblong, noncircular foundations should be increased in accordance with the results of Dobry and Gazetas (1986) to account for the more efficient emission of waves from oblong foundations.

Foundation Flexibility

Impedance functions for flexible circular foundation slabs supporting shear walls have been evaluated for a number of wall configurations, including the following: (1) Rigid core walls (Iguchi and Luco 1982); (2) thin perimeter walls (Liou and Huang 1994); and (3) rigid concentric interior and perimeter walls (Riggs and Waas 1985). These studies focused on the effects of foundation flexibility of rocking impedance; the horizontal impedance of flexible and rigid foundations are similar (Liou and Huang 1994). Foundation flexibility effects on rocking impedance are most significant for a rigid central core with no perimeter walls. For this case, the flexible foundation has significantly less stiffness and damping than the rigid foun-

dation. The reductions are most significant for narrow central cores and large deviations between soil and foundation slab rigidity. Hence, corrections for foundation flexibility effects should be made to rocking impedance terms for structures having central core shear walls in accordance with the analytical results of Iguchi and Luco (1982). Use of the rigid foundation assumption introduces much smaller errors to rocking impedance terms for other wall configurations.

Piles or Piers

The influence of pile foundations on impedance functions cannot easily be accounted for with simplified analyses. Many analytical techniques are available for evaluating the impedance of pile supported foundations [e.g., Novak (1991) and Gohl (1993)], but a review of such techniques is beyond the scope of this paper. The effects of piles/piers was not directly included in the development of impedance functions for the analyses presented in the companion paper (Stewart et al. 1999). Instead, the influence of foundation type on the final results was evaluated empirically.

Effects of Inertial SSI on Buildings

Veletsos and Meek (1974) found that the maximum seismically induced deformations of a single-degree-of-freedom model of a structure with a surface foundation can be predicted accurately by an equivalent fixed-base single-degree-of-freedom oscillator with period $\tilde{T}$ and damping ratio $\tilde{\zeta}$. These are referred to as "flexible-base" parameters, because they represent the properties of an oscillator that is allowed to translate

and rotate at its base. The flexible-base period is evaluated from (Veletsos and Meek 1974),

$$\frac{\tilde{T}}{T} = \sqrt{1 + \frac{k}{k_u} + \frac{kh^2}{k_\theta}} \qquad (5)$$

where T = fixed-base period of the structure in Fig. 1 ($\sqrt{k/m}$). The flexible-base damping ratio has contributions from viscous damping in the structure as well as radiation and hysteretic damping in the foundation. Veletsos and Nair (1975) expressed the flexible-base damping $\tilde{\zeta}$ as

$$\tilde{\zeta} = \tilde{\zeta}_0 + \frac{\zeta}{(\tilde{T}/T)^3} \qquad (6)$$

where $\tilde{\zeta}_0$ is referred to as the foundation damping factor and represents the damping contributions from foundation-soil interaction (with hysteretic and radiation components); and ζ = fixed-base damping ratio. A closed-form expression for $\tilde{\zeta}_0$ is represented in Veletsos and Nair (1975). Bielak (1975) similarly expressed the effects of inertial interaction for embedded structures in terms of period lengthening ratio $\tilde{T}/T$ and foundation damping factor $\tilde{\zeta}_0$.

For both the Veletsos and Nair (1975) and Bielak (1975) formulations, the relationships between the fixed- and flexible-base structure properties depend on aspect ratio h/r_θ, soil Poisson ratio ν, soil hysteretic damping ratio β, and the following dimensionless parameters:

$$\sigma = V_S T/h \qquad (7)$$

$$\gamma = \frac{m}{\rho \pi r_u^2 h} \qquad (8)$$

where σ and γ = measures of the ratio of the soil-to-structure stiffness and structure-to-soil mass, respectively. For most conventional building structures, $\sigma > 2$ and $\gamma \approx 0.1-0.2$ [a representative value of $\gamma = 0.15$ is recommended by Veletsos and Meek (1974)]. Both $\tilde{T}/T$ and $\tilde{\zeta}_0$ are sensitive to σ, while the sensitivity to γ is modest for $\tilde{T}/T$ ($\pm 10-15\%$ variation across reasonable range of γ) and low for $\tilde{\zeta}_0$ (Aviles and Perez-Rocha 1996).

For the case of rigid, circular foundations founded on, or embedded into, a viscoelastic half-space, analytical results from Veletsos and Nair (1975) and Bielak (1975) for $\tilde{T}/T$ and $\tilde{\zeta}_0$ versus $1/\sigma$ are shown in Fig. 3. The static foundation stiffnesses were modified according to (4) for application of the Veletsos and Nair model to embedded foundations. These results indicate that the ratio of structure-to-soil stiffness $1/\sigma$ is a critical factor controlling the period lengthening. In addition, for a given value of $1/\sigma$, $\tilde{T}/T$ increases for structures with increasing aspect ratio and decreasing embedment. The flexible-base damping $\tilde{\zeta}$ can increase or decrease relative to fixed-base damping ζ depending on the period lengthening and the foundation damping factor $\tilde{\zeta}_0$. As shown in Fig. 3, $\tilde{\zeta}_0$ increases with $1/\sigma$ and embedment ratio and decreases with aspect ratio.

A comparison of the analytical results from the two formulations indicates essentially identical results for surface foundations ($e/r = 0$). For the case of $e/r = 1$, increases in damping and decreases in period lengthening are predicted by
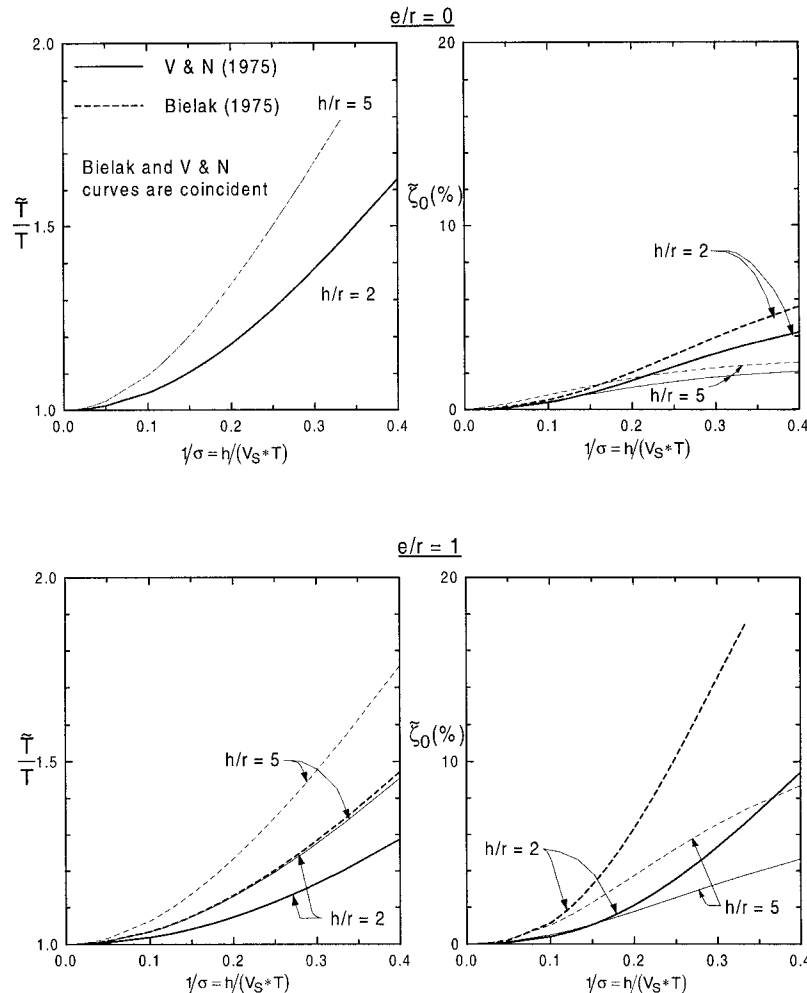

FIG. 3. Comparison of Period Lengthening Ratios and Foundation Damping Factors for Single-Degree-of-Freedom Structure with Rigid Circular Foundation on Half-Space for Surface and Embedded Foundations ($\nu = 0.45$, $\beta = 5\%$, $\gamma = 0.15$, $\zeta = 5\%$) (Veletsos and Nair 1975; Bielak 1975)

both models, although the Veletsos and Nair approach yields lower predictions of $\tilde{T}/T$ and $\tilde{\zeta}_0$. It should be noted that the embedment ratio $e/r = 1$ is approaching the limit of validity for the expression in (4), and results from the two formulations are more consistent for lower e/r.

Summary of Analysis Procedures

For analysis of inertial interaction effects, the objectives are predictions of first-mode period lengthening ratio $\tilde{T}/T$ and foundation damping factor $\tilde{\zeta}_0$. As shown in Fig. 4(a), the motivation for characterizing these inertial interaction effects is that they can be used to estimate flexible-base modal parameters $\tilde{T}$ and $\tilde{\zeta}$, which in turn are used in response spectrum-based approaches for evaluating design-level seismic base shear forces and deformations in structures.

The parameters needed for analysis of $\tilde{T}/T$ and $\tilde{\zeta}_0$ are as follows:

- *Soil Conditions:* Shear-wave velocity V_S and hysteretic damping ratio β that are representative of the site stratigraphy and the level of ground shaking; representative soil Poisson's ratio ν.
- *Structure/Foundation Characteristics:* Effective height of structure above foundation level h; embedment e; foundation radii that match the area and moment of inertia of the actual foundation r_u and r_θ, respectively; appropriate corrections to the foundation impedance for embedment, shape, and flexibility effects.
- *Fixed Base First-Mode Parameters:* Period and damping ratio, T and ζ, respectively.

Using these data, the following steps are carried out:

1. Evaluate the impedance function at an assumed period for the flexible-base structure $\tilde{T}$. Static foundation stiffnesses are computed first according to (3) with appropriate modifications for embedment effects [(4)]. Dynamic coefficients α_u, α_θ, β_u, and β_θ are then evaluated for the assumed $\tilde{T}$ using equations in Veletsos and Verbic (1973) with appropriate modifications to β_θ to account for foundation shape effects and to α_θ and β_θ to account for flexible foundation effects.
2. Calculate dimensionless parameters σ and γ using (7) and (8). Lacking more precise information, it is assumed that $\gamma = 0.15$.

3. Estimate $\tilde{T}/T$ and $\tilde{\zeta}$ using (5) and (6) and calculate a new estimate of $\tilde{T}$.
4. Repeat Steps 1–3 until the dynamic coefficients α_u, α_θ, β_u, and β_θ are estimated at $\tilde{T}$.
5. For embedded foundations, repeat the analyses for $\tilde{T}/T$ and $\tilde{\zeta}_0$ using the formulation by Bielak (1975).

The procedures in Steps 1–4 are referred to as the "modified Veletsos" (MV) formulation. The modified term refers to the extension of the basic model considered in Veletsos and Nair (1975) to account for embedded, noncircular, and flexible foundations and nonuniform soil profiles. Similarly, the Bielak (1975) procedure applied in Step 5 to embedded structures is referred to as the "modified Bielak" (MB) formulation.

Example

Application of the modified Veletsos and Bielak analysis procedures is illustrated for a six-story office building in Los Angeles, Calif. The building structure and site conditions are illustrated in Figs. 5(a and b). The lateral force resisting system is concentrated in four towers at the building corners. The towers are steel-braced frames and moment-resisting frames and are founded on independent 1.2–1.5-m-thick mat foundations. The analyses performed here pertain to the east-west response of the building's west tower, and foundation parameters are defined for the rectangular mat supporting this tower (10.5 × 12.7 m in plan). Site conditions consist of ~15 m of silty, gravelly sand overlying stiffer clayey and gravelly soils. The shear-wave velocity V_S profile in Fig. 5(b) was derived from downhole cone penetration testing to a depth of 6 m (where refusal of the cone penetration test probe was encountered) and interpretations of surface wave measurements by Rodriquez-Ordonez (1994). V_s values from the surface wave measurements are given little weight near the ground surface and at depths $\gtrsim$ 15 m due to systematic errors in these data noted by Boore and Brown (1998). The peak ground acceleration in the free-field at the site during the Northridge earthquake was 0.25g (Todorovska 1996).

The analysis begins by characterizing the soil, foundation, and structure conditions. The soil is modeled as a half-space, despite the significant impedance contrast at a depth of ~15 m. The modeling is justified by the relatively small foundation radii for the mat foundation (r_u = 6.5 m, r_θ = 6.3 m), which are less than half of the depth to the stiffer soil layer. Based on the V_S profile in Fig. 5(b), the averaged small strain shear-wave velocity for the half-space is 240 m/s (for an effective
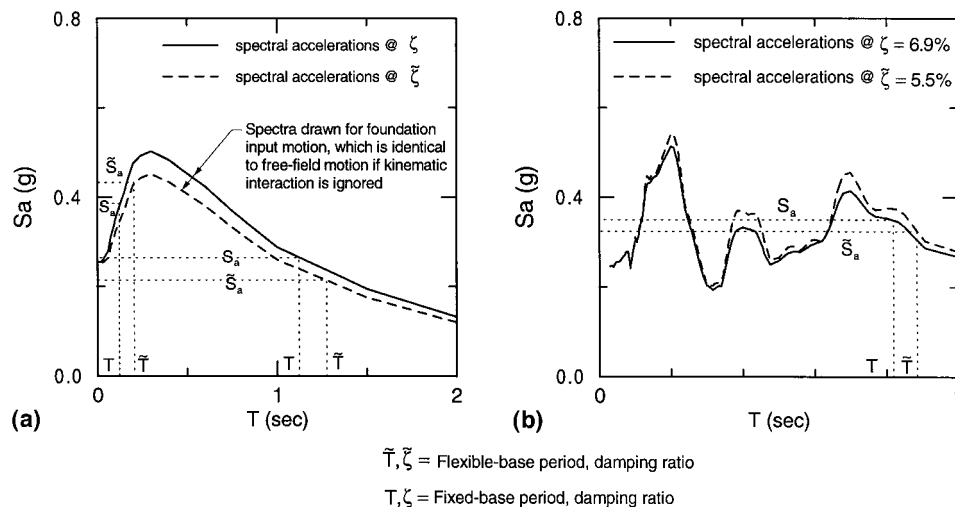

FIG. 4. (a) Schematic Showing Effects of Period Lengthening and Foundation Damping on Design Spectral Acceleration Using Smoothed Spectral Shape — S_a Can Increase or Decrease Due to SSI; (b) Effect of Period Lengthening and Foundation Damping on S_a at Site A23

$\tilde{T}, \tilde{\zeta}$ = Flexible-base period, damping ratio
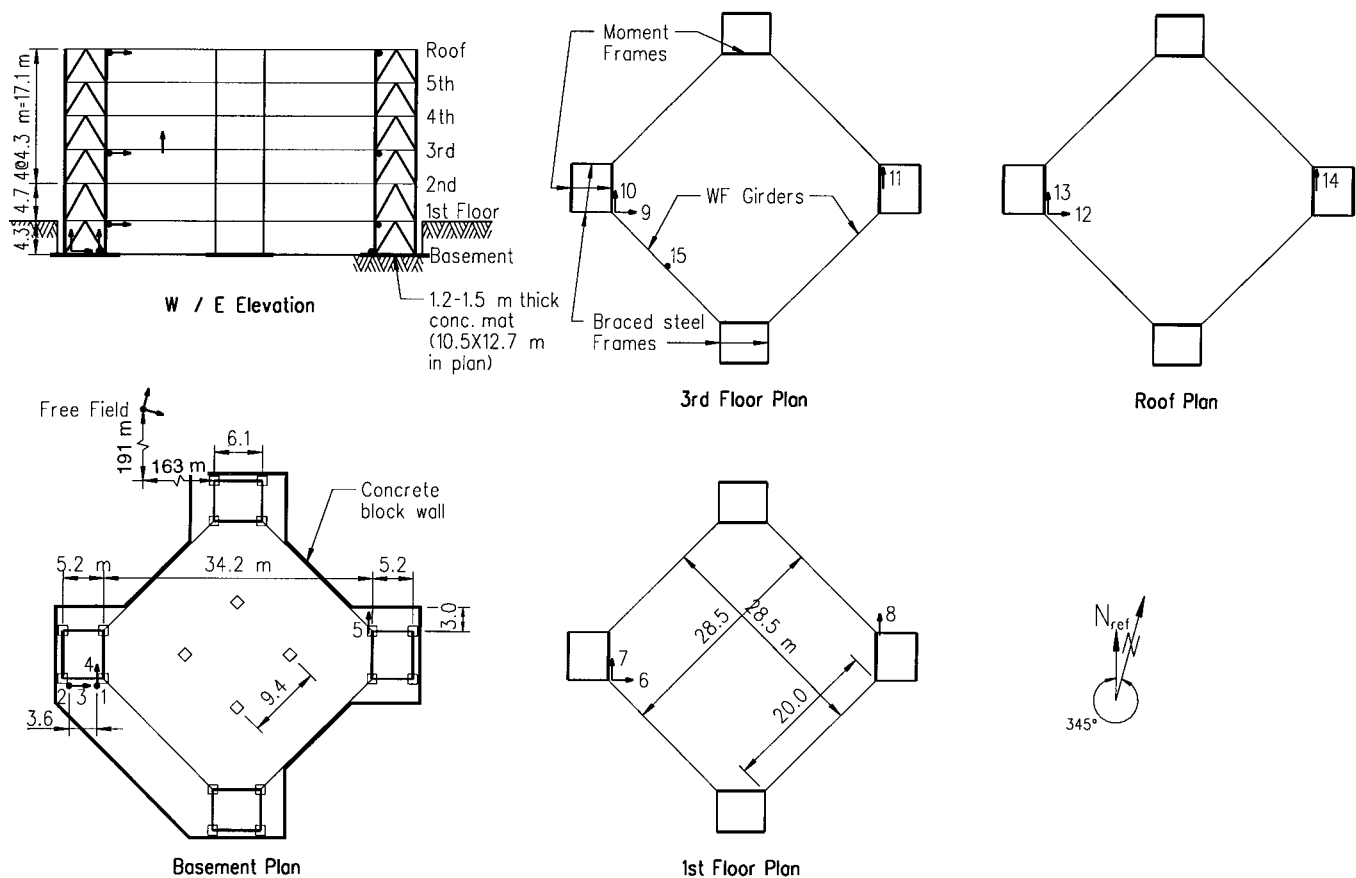
T, ζ = Fixed-base period, damping ratio

FIG. 5(a). Sensor Locations and Structural Configuration at Los Angeles Six-Story Office Building (Note: Data Provided by California Strong Motion Instrumentation Program)
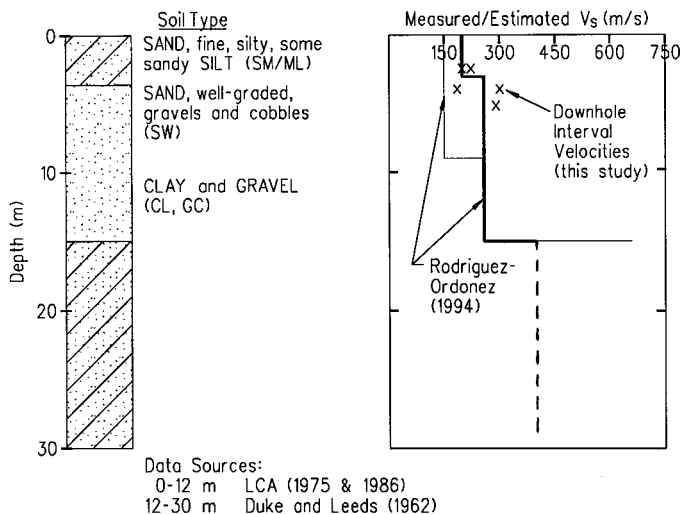

FIG. 5(b). Generalized Soil Column at Los Angeles Six-Story Office Building [Data Sources: 0–12 m (LCA, Confidential Reports, 1975 and 1986); 12–30 m (Duke and Leeds 1962)]

profile depth of 10.8 m). A deconvolution analysis is performed with the one-dimensional site response analysis program SHAKE (Schnabel et al. 1972) using the recorded free-field motion (peak acceleration = 0.25g) and the profile in Fig. 5(b). This analysis indicates shear strain compatible effective half-space parameters V_S = 190 m/s and β = 5.2%. The foundation is modeled as a rigid disk embedded 4.3 m into the soil, although it is noted that the foundation walls are not continuous around the foundation perimeter. No adjustments to the impedance function are made for foundation flexibility or shape effects. The tower is modeled as a single-degree-of-freedom system with a height of 17 m (~2/3 of the overall

building height) and a normalized mass γ = 0.15. From system identification analyses (discussed in the following section) the fixed-base first-mode period is T = 0.81 s. Combining these data indicates an east-west structure-to-soil stiffness ratio of 1/σ = 0.11.

Based on the foregoing characterization of soil, foundation, and structure properties, the first-mode period lengthening and foundation damping are predicted to be $\tilde{T}/T$ = 1.04 and 1.06 and $\tilde{\zeta}_0$ = 0.5 and 1.2% by the MV and MB formulations, respectively. These predictions are compared to system identification results in the following section.

EVALUATION OF SOIL-STRUCTURE INTERACTION EFFECTS USING SYSTEM IDENTIFICATION ANALYSES

Overview of System Identification

As illustrated schematically in Fig. 6(a), the objective of system identification analyses is to evaluate the unknown properties of a system using a known input into, and output from, that system. For analyses of seismic structural response, the "system" has an unknown flexibility that generates a known difference between pairs of input and output strong motion recordings. For example, as indicated in Fig. 6(b), parameters describing the fixed-base system are evaluated from input/output pairs that differ only by the structural deformation u. Likewise, parameters describing the flexible base system are evaluated from strong motion pairs whose difference results from foundation flexibility in translation u_f and rocking θ, as well as structural flexibility. A comparison of fixed- and flexible-base modal parameters provide a direct quantification of SSI effects.

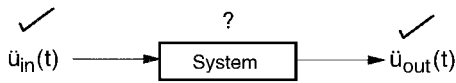There are two principal system identification procedures:

FIG. 6(a). Schematic of System Identification Problem

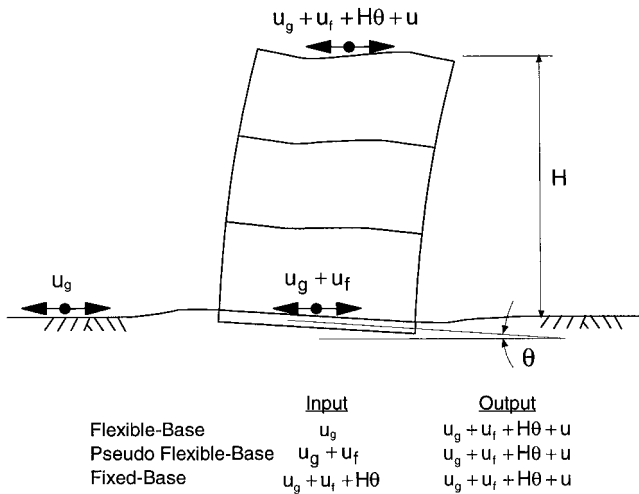|	Input	Output
Flexible-Base	u_g	$u_g + u_f + H\theta + u$
Pseudo Flexible-Base	$u_g + u_f$	$u_g + u_f + H\theta + u$
Fixed-Base	$u_g + u_f + H\theta$	$u_g + u_f + H\theta + u$

FIG. 6(b). Motions Used as Inputs and Outputs for System Identification of Structures

1. Nonparametric procedures evaluate complex-valued transmissibility functions from the input and output recordings without fitting an underlying model. These transmissibility functions represent an estimate of the ratio of output to input motion in the frequency domain and are computed from smoothed power and cross-power spectral density functions of the input and output motions. Modal frequencies and damping ratios are estimated from peaks in the transmissibility function amplitude (Pandit 1991; Ljung 1987; Fenves and DesRoches 1994).

2. Parametric procedures develop numerical models of transfer functions, which represent the ratio of output to input motion in the Laplace domain. The amplitude of the transfer function is a surface in the Laplace domain. Peaks on this surface are located at poles which can be related to modal frequencies and damping ratios. Parameters describing transfer function models are estimated by minimizing the error between the model output and recorded output in the discrete time domain using least-squared techniques. The transfer function surface can be estimated by minimizing cumulative error for the entire time history (Safak 1991a) or by recursively minimizing error for each time step using a window of time immediately preceding that time step (Safak 1991b).

The evaluation of vibration frequencies and damping ratios from transmissibility functions can be problematic (especially for damping), because the shape of the functions is dependent on details associated with the computation of the spectral density functions such as the number of points in the fast Fourier transform and the windowing procedures used (Pandit 1991). Parametric procedures provide a relatively rigorous modeling of system response, because the transfer function for a given set of time histories is only dependent on two user-defined parameters: (1) The delay between the input and output; and (2) the number of modes used in the analyses (i.e., the order of the model). When these parameters are selected judiciously, the modal frequencies and damping ratios can be reliably evaluated for linear structures. Hence, parametric identification techniques were used for the evaluation of structural modal vibration parameters in this study.

Evaluation of Modal Parameters for Various Base Fixity Conditions

Three cases of base fixity are of interest in analyses of SSI: (1) Fixed-base, representing only the flexibility of the structure; (2) flexible-base, representing the combined flexibility of the complete soil-structure system; and (3) pseudoflexible-base, representing flexibility in the structure and rocking in the foundation. Pseudoflexible-base parameters are of interest because they can sometimes be used as direct approximations of flexible-base parameters or to estimate either fixed- or flexible-base parameters.

Stewart and Fenves (1998) evaluated the types of input and output strong motion recordings that are necessary to evaluate fixed-, flexible-, and pseudoflexible-base vibration parameters of structures with parametric identification procedures. While roof translations are always used as output, the input motions for various base fixity conditions vary as indicated in Fig. 6(b). Recordings of free-field, foundation, and roof level translations, as well as base rocking, are needed to evaluate directly both fixed- and flexible-base modal parameters of a structure.

Instrumented buildings often lack sensors for recording base rocking or free-field translations. For such cases either fixed-base parameters (missing base rocking) or flexible-base parameters (missing free-field translations) cannot be evaluated directly from system identification analyses. Stewart and Fenves (1998) derived expressions to estimate either flexible- or fixed-base parameters using known modal parameters for the two other cases of base fixity. The estimation procedures operate on the premise that differences between known parameters can be used to calibrate the foundation impedance at the structure's period; the calibrated impedance can then be used to estimate the unknown parameters. These estimation procedures extend the number of sites for which SSI effects can be empirically evaluated. Only 11 sites considered in the companion paper have complete instrumentation sets, but the estimation procedures enable SSI effects to be evaluated for an additional 46 sites.

Application of System Identification Procedures

In this section, modal vibration parameters for the previously discussed six-story office building are evaluated using parametric system identification procedures. The free-field, foundation-level, and roof translations were recorded as well as base rocking, so that both fixed- and flexible-base modal parameters can be identified. Selected strong motion recordings from the site are shown in the upper three frames of Fig. 7. Parametric system identification was performed to estimate flexible-, pseudoflexible, and fixed-base parameters in the east/west direction. The identification procedure is comprised of the following steps, which are illustrated using the roof/free-field (flexible-base) pair.

1. Two user-defined parameters are needed to define the parametric model: The time delay d, between the input and output motions, and the number of modes necessary to optimize the response J. The delay is evaluated by examining the variation of cumulative error between the recorded output and model output as a function of d using a single mode, that is, $J = 1$. The value that minimizes the error for the example structure is $d = 2$ time steps, as shown in Fig. 8. Using this delay, the model order is estimated by calculating the variation of error with J. Fig. 9 shows that the error initially decreases rapidly with J, but stabilizes beyond a value of $J = 4$, which is the selected model order.

2. Using these d and J values, parameters describing the transfer function surface are calculated by minimizing
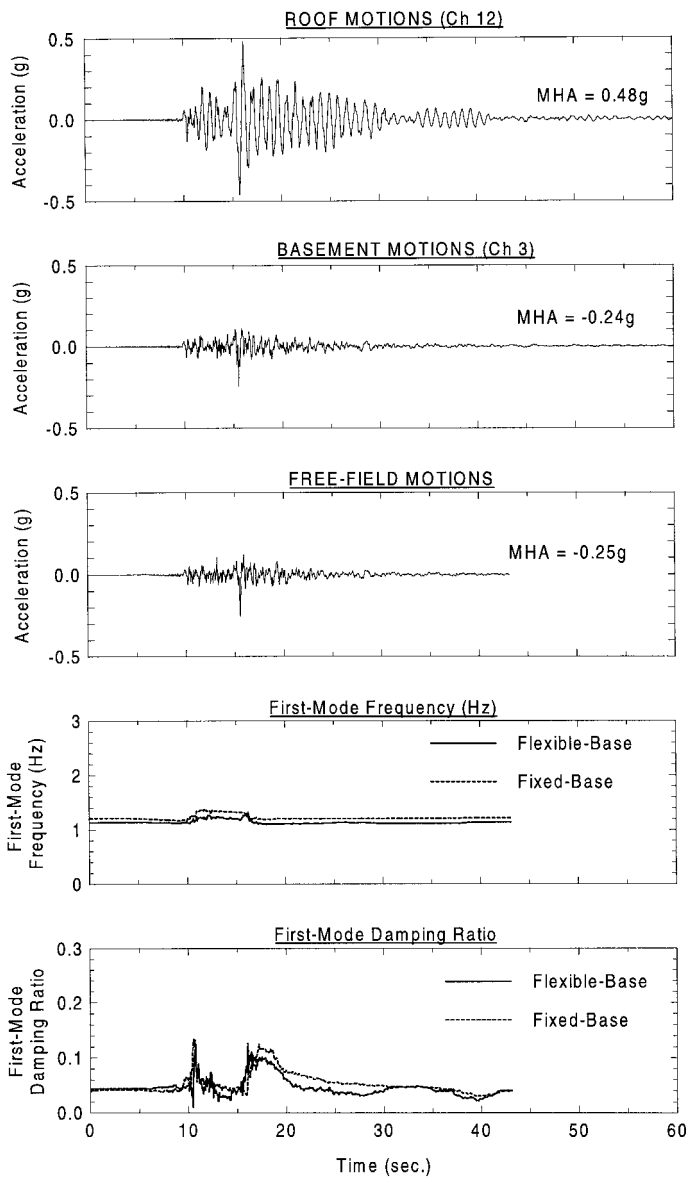
FIG. 7. East/West Acceleration Time Histories and Time Variation of First-Mode Parameters, Los Angeles Six-Story Office Building, 1994 Northridge Earthquake
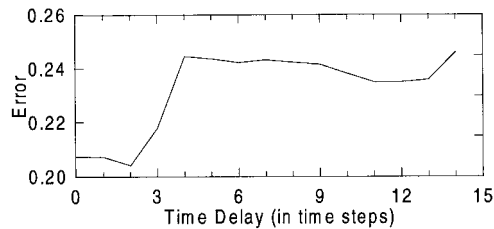

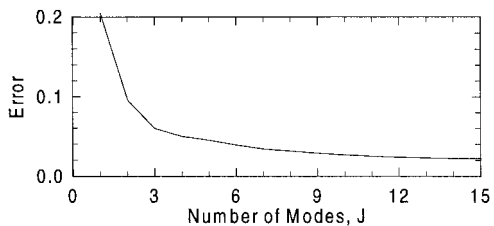FIG. 8. Variation of Error with Time Delay

FIG. 9. Variation of Error with Number of Modes

the cumulative error between the model output and recorded output using a least-squared technique [this is termed the cumulative error method (CEM)]. These parameters are used to define a transfer function surface with "poles" (high points) and "zeros" (low points). Modal frequencies ω_j and damping ratios ζ_j can be computed from the complex-valued pole locations s_j as follows (Stewart and Fenves 1998):

$$s_j, s_j^* = \zeta_j\omega_j \pm i\omega_j\sqrt{1 - \zeta_j^2} \qquad (9)$$

Fig. 10 presents the flexible-base transfer function surface for the example structure with the axes on the horizontal plane scaled according to (9) to match the modal frequency and damping at the poles.

3. The intersection of the model transfer function surface with the imaginary plane is compared to the nonparametric transmissibility function amplitude to check the model. Major peaks of the curves should occur at similar frequencies, but the amplitude match is not always good because the transmissibility function amplitudes are somewhat arbitrary due to their dependence on the smoothing technique used and the number of points in the fast Fourier transform. As shown in Fig. 11, a good

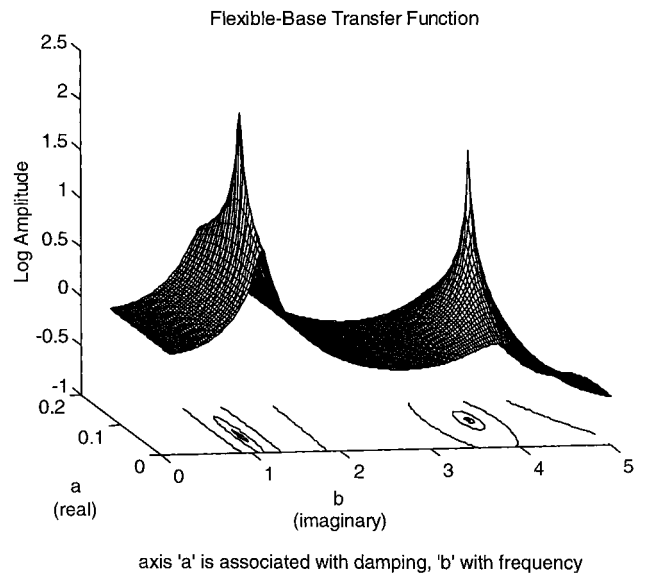axis 'a' is associated with damping, 'b' with frequency

FIG. 10. Flexible-Base Transfer Function Surface Identified by Parametric System Identification, Los Angeles Six-Story Office Building, 1994 Northridge Earthquake
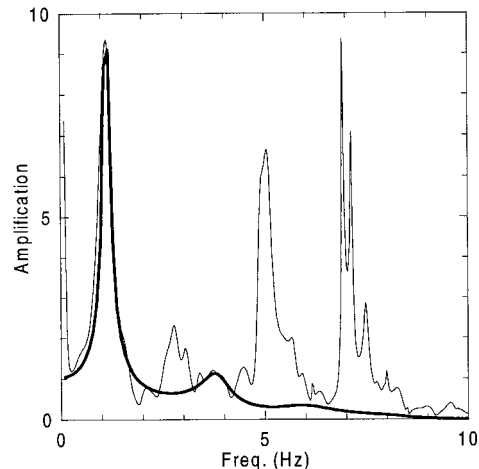

FIG. 11. Comparison of Transmissibility Functions from Nonparametric Analysis (Light Line) and Parametric Model (Heavy Line)

match is obtained near the first-mode frequency. The match is poor at higher frequencies, indicating the limited ability of transmissibility functions to capture higher mode responses containing relatively little seismic energy.

4. Additional checks on the parametric identification are performed as follows: First, the unscaled poles and zeros of the transfer function are plotted in the complex plane to check for pole-zero cancellation (Fig. 12). The pole locations (s_j) in Fig. 12 are the unscaled counterparts to the pole locations on the horizontal plane in Fig. 10. The unscaled poles should always plot inside the unit circle, whereas zeros can be inside or outside the circle. If poles and zeros are found to overlap, the model is overconstrained and J is decreased. Second, the model and recorded outputs are compared, and the residual is computed (Fig. 13). This check is made to confirm that the residual is small compared to the recorded output, and that the residual has no dominant frequencies. Third, the cross-correlation of the residual with the input is computed to determine if there are components common to these time series (Fig. 14). The dashed lines in Fig. 14 are the 99% confidence intervals of independence, meaning that there is a 99% probability that the cross-correlation will be contained within these limits if the residual and input are truly independent. Significant cross-correlation indicates that the model order should be increased to better define the transfer function (Safak 1991a). However, high cross-correlation at negative lags is common
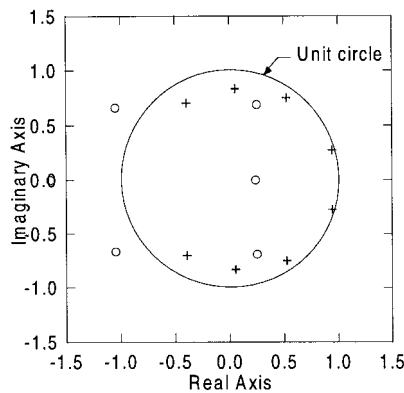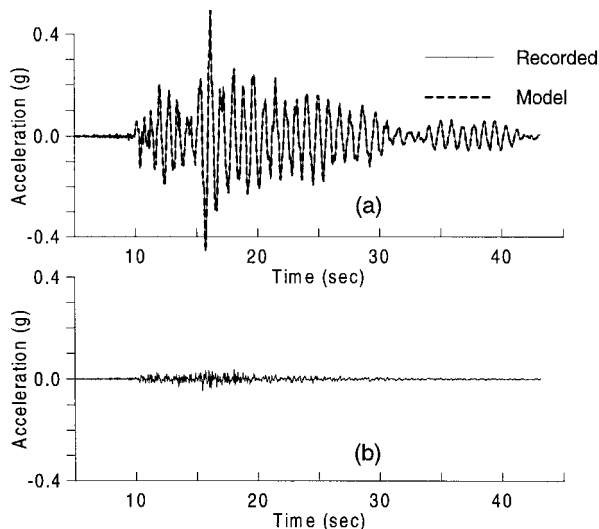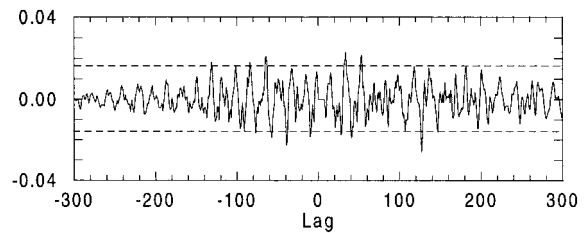

FIG. 14. Cross-Correlation Function between Input and Residual and 99% Confidence Limits of Independence

TABLE 1. Results of CEM Parametric Analyses for Response of Los Angeles Six-Story Office Building, 1994 Northridge Earthquake

Mode (1)	$\tilde{f}$ (Hz) (2)	$\tilde{\zeta}$ (%) (3)	$\tilde{f}*$ (Hz) (4)	$\tilde{\zeta}*$ (%) (5)	f (Hz) (6)	ζ (%) (7)
1	1.12 ± 0.01	5.5 ± 0.5	1.11 ± 0.01	6.6 ± 0.4	1.21 ± 0.01	6.9 ± 0.5
2	3.85 ± 0.05	8.4 ± 1.0	3.83 ± 0.03	8.5 ± 0.5	3.83 ± 0.03	7.4 ± 0.7

TABLE 2. Empirical and Predicted Inertial Interaction Effects

(1)	$\tilde{T}/T$ (2)	$\tilde{\zeta}_0$ (%) (3)
System identification (CEM)	1.08	0.0
MV Prediction	1.04	0.5
MB Prediction	1.06	1.2

and indicates output feedback in the input (Ljung 1987). This is a product of SSI and does not imply a problem with the model.

5. The nonlinearity of the structural response can be investigated using the time variability of first-mode parameters calculated by recursive parametric identification (Safak 1991b). These analyses are performed using the d and J values from Step 1. Plots of the time-dependent first-mode frequencies and damping ratios for the example pair are presented in Fig. 7, from which an essentially time invariant first-mode response is observed.

Modal frequencies and damping ratios computed by the CEM for the example structure are shown in Table 1. The standard errors of the modal parameters are associated with random disturbances in the data. These data indicate a period lengthening ratio of $\tilde{T}/T = 1.08$ and a foundation damping factor of $\tilde{\zeta}_0 = 0$. As shown in Fig. 4(b), these SSI effects decrease the spectral acceleration at the first-mode period relative to what would have occurred in a fixed-base structure.

The "empirical" $\tilde{T}/T$ and $\tilde{\zeta}_0$ values are compared to estimates from predictive analysis procedures in Table 2. The estimates by both procedures are reasonably good considering the limited availability of good quality V_S data. However, it may be noted that the MB model slightly overpredicts $\tilde{\zeta}_0$ values relative to the MV model. This likely results from the lack of continuity of the basement walls around the tower's mat foundation.

Interpretation of System Identification Results for Evaluating SSI Effects

A rational interpretation of fixed- and flexible-base modal parameters from multiple sites requires an assessment of relative confidence levels in the results and assessments of the effects of numerical errors or system nonlinearities on the

FIG. 12. Zeros (○) and Poles (+) of Discrete-Time Transfer Function

**FIG. 13. (a) Comparison of Model and Recorded Output; (b) Residual of Identification for Roof Motions**

identifications. The handling of these issues is the focus of this section.

Confidence Levels

System identification results for sites considered in this study are assigned one of three possible confidence levels: A = acceptable confidence, L = low confidence, and U = unacceptable confidence. Unacceptable confidence is associated with one of the following situations:

- U1: Reliable flexible-base parameters could not be developed due to significant incoherence between foundation and free-field motions.
- U2: The structure was so stiff that the roof and foundation level motions were essentially identical, and hence the response could not be established by system identification.
- U3: For the A sites, fixed-base parameters could not be obtained directly from system identification and also could not be estimated because $\tilde{T} < \tilde{T}^*$ and base rocking effects were evident from comparisons of vertical foundation and free-field motions. Evidence of base rocking suggests that SSI effects are significant, and that fixed-base period will differ substantially from flexible- and pseudoflexible-base period. Hence, the inability to estimate the fixed-base period necessarily terminates the analysis. Similarly, at the B sites, flexible-base parameters could not be estimated because $T > \tilde{T}^*$.
- U4: Reliable parametric models of structural response could not be developed for unknown reasons.

Low confidence levels occur most often because of poor characterization of geotechnical conditions (i.e., insufficient in-situ data to evaluate stratigraphy and shear-wave velocities to depths of about one foundation radius). Although geotechnical data have no direct effect on vibration parameters evaluated through system identification, V_s affects the manner in which SSI results are interpreted relative to other sites through the parameter σ [(7)]. Other reasons for low confidence in the results include contamination of free-field motions from vibrations of nearby structures, moderately incoherent foundation and free-field motions, and short duration strong motion data.

Errors in First-Mode Parameters

There is always uncertainty in models identified from parametric analyses due to imperfect model structures and disturbances in the output data (Ljung 1995). Systematic errors can result from inadequate model structure (i.e., poor selection of the d or J parameters) that cannot be readily quantified. A second type of error results from random disturbances in the data. This error quantifies how the model would change if the identification were repeated with the same model structure and input but with a different realization of the output. This uncertainty can be readily computed from the least-squares solution for the model parameters. The coefficients of variation associated with random disturbance errors are generally about 0.5–1.5% for frequency and 5–15% for damping.

Errors associated with inadequate model structure are controlled by selecting J to minimize deviations between the model output and roof recording, while not overparameterizing the model in such a way as to cause pole-zero cancellation in the transfer function. However, an additional constraint is a need to maintain the same J for all output/input pairs in a given direction. This is enforced to maximize the likelihood that variations between modal parameters for different conditions of base fixity are reflective of true SSI effects and not

by-products of the analysis. As a result of this constraint on J, models for some output/input pairs may not be optimally parameterized with respect to the minimization of model error.

Despite these efforts to develop consistent models for different input/output pairs, numerical errors can still occur that result in conditions such as $\tilde{T} < \tilde{T}^*$ or $\tilde{\zeta}_0 < 0$. Such errors are generally small (i.e., within the range of the random errors noted earlier) and only become apparent at sites where inertial interaction effects are small. Nonetheless, the $\tilde{T} < \tilde{T}^*$ condition makes impossible the implementation of fixed-base parameter estimation procedures in Stewart and Fenves (1998). In such cases, the significance of base rocking is evaluated using foundation-level and free-field vertical motions and one of the following is done: (1) If rocking is evident from amplification of foundation-level vertical motions at the fundamental mode of the structure, the results for the site are discarded (see error U3 earlier); or (2) if no rocking is evident, fixed-base parameters are approximated by pseudoflexible-base parameters. Hence, the results for some sites indicate $\tilde{T} < T$, despite the obvious error associated with such a finding. Similarly, there are cases of $\tilde{\zeta}_0 < 0$. Such results are interpreted as indicative of small SSI effects and are taken as $\tilde{T}/T = 1$ or $\tilde{\zeta}_0 = 0$.

System Nonlinearities

Modal parameters are generally developed from CEM parametric system identification analyses and, hence, are based on the assumption of linear, time invariant behavior. As a check of this assumption, the time dependence of first-mode parameters are also evaluated by recursive techniques. An example of essentially linear, time invariant response was previously provided in Fig. 7. An illustration of nonlinear structural response is provided by the six-story Imperial County Service Building (ICSB), which partially collapsed during the 1979 Imperial Valley earthquake. As shown in Fig. 15, reductions in first-mode frequency and high damping are evident during the first 20 s of strong shaking. A nonlinear structural response can lead to significant differences between modal parameters at a given time and CEM modal parameters evaluated across the duration of the time history. What is important from the standpoint of evaluating inertial interaction effects is that differences between CEM parameters for different cases of base fixity are consistent with differences in recursive parameters during times when the identification is stable. For example, at the ICSB, differences between fixed- and pseudoflexible-base frequencies were generally consistent with the difference in CEM frequencies throughout the duration of strong shaking (CEM results were $\tilde{f} = 1.36$, $\tilde{f}^* = 1.54$ Hz). Conversely, differences between damping values were strongly time-dependent, with $\tilde{\zeta}$ significantly exceeding $\tilde{\zeta}^*$ for $t < 20$ s and the opposite trend subsequently. The corresponding CEM results are $\tilde{\zeta} = 16.8\%$ and $\tilde{\zeta}^* = 13.5\%$, which is reasonably representative of recursive results during early portions of the time history. Recursive results for $t < 20$ s are more stable than subsequent results due to the much reduced amplitude of shaking for $t > 20$ s. Hence, the CEM damping results were consistent with recursive results from the most stable portion of the time history in this case, and the CEM results were used for final characterization of SSI effects at the site.

Occasionally, the differences between modal parameters from CEM and recursive analyses are inconsistent. In such cases, average differences between parameters for different base fixity conditions computed from recursive analyses over times of stable identification can be used for evaluating SSI effects. Such usage of recursive results was seldom necessary but was more common for evaluating $\tilde{\zeta}_0$ than $\tilde{T}/T$. These corrections, where made, are indicated in Stewart and Stewart (1997).
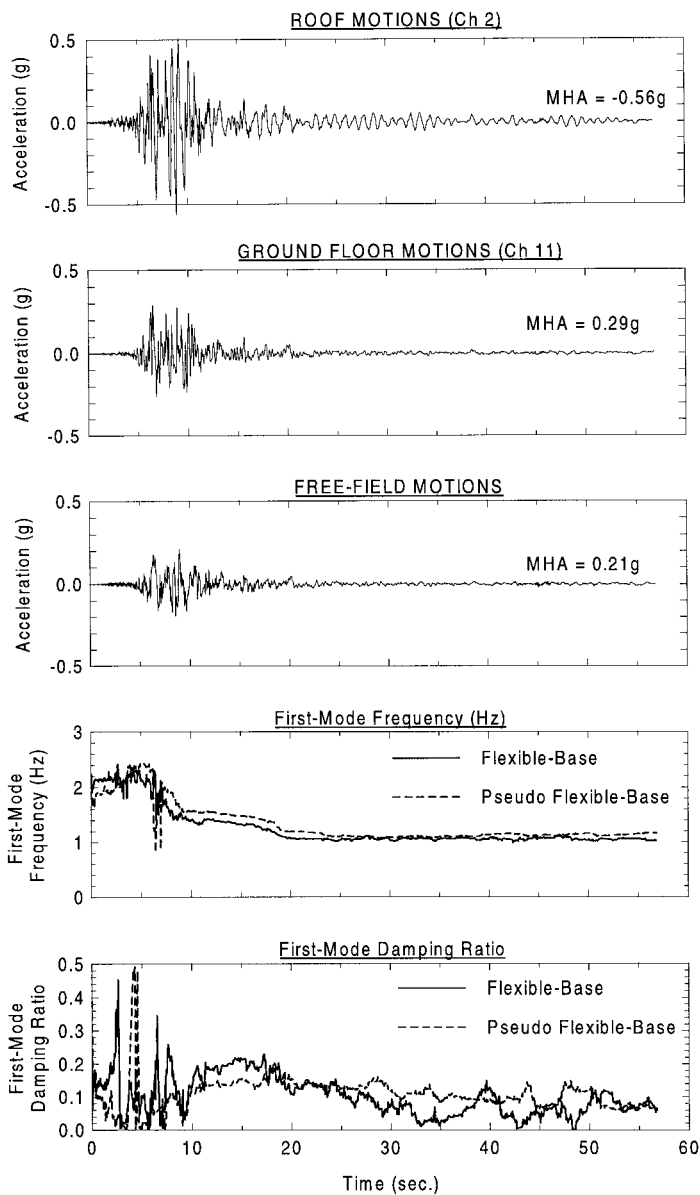
FIG. 15. Transverse Acceleration Time Histories and Time Variation of First-Mode Parameters, ICSB, 1979 Imperial Valley Earthquake

CONCLUSIONS

Two sets of analyses are described in this paper: (1) Simplified design procedures that can be used to predict period lengthening ratios and foundation damping factors for structures with surface (MV) or embedded (MV or MB) foundations; and (2) system identification procedures for evaluating fixed- and flexible-base modal vibration parameters from earthquake strong motion data.

The greatest uncertainty in use of the MV and MB procedures for a given free-field motion is associated with the impedance function. Careful consideration must be given to evaluation of the shear-wave velocity profile, the modeling of embedded foundations (the MB procedure may not be appropriate if basement walls are not continuous around the foundation perimeter), oblong foundations, or flexible foundations supporting a central core of stiff shear walls.

Parametric system identification procedures provide a reliable basis for evaluating modal vibration parameters in structures for different base fixity conditions. However, rational interpretation of the results from such analyses requires due consideration of potential numerical errors in the identification

due to disturbances in the strong motion data and proper characterization of nonlinear structural response.

APPENDIX I. REFERENCES

Applied Technology Council (ATC). (1978). "Tentative provisions for the development of seismic regulations for buildings: A cooperative effort with the design profession, building code interests, and the research community." *Rep. No. ATC 3-06*, U.S. Dept. of Commerce, National Bureau of Standards, Washington, DC.

Apsel, R. J., and Luco, J. E. (1987). "Impedance functions for foundations embedded in a layered medium: An integral equation approach." *J. Earthquake Engrg. Struct. Dyn.*, 15(2), 213–231.

Aviles, J., and Perez-Rocha, L. E. (1996). "Evaluation of interaction effects on the system period and the system damping due to foundation embedment and layer depth." *Soil Dyn. and Earthquake Engrg.*, 15(1), 11–27.

Bielak, J. (1975). "Dynamic behavior of structures with embedded foundations." *J. Earthquake Engrg. Struct. Dyn.*, 3(3), 259–274.

Boore, D. M., and Brown, L. T. (1998). "Comparing shear-wave velocity profiles from inversion of surface-wave velocities with downhole measurements: Systematic differences between the CXW method and downhole measurements at six USC strong motion sites." *Seism. Res. Letters*, 69(3), 222–229.

Building Seismic Safety Council (BSSC). (1997). "NEHRP recommended provisions for seismic regulations for new buildings, Part 1, Provisions and Part 2, Commentary. *Rep. No. FEMA 302 and 303*, Federal Emergency Management Agency, Washington, D.C.

Dobry, R., and Gazetas, G. (1986). "Dynamic response of arbitrarily shaped foundations." *J. Geotech. Engrg.*, ASCE, 112(2), 109–135.

Duke, C. M., and Leeds, D. J. (1962). "Site characteristics of southern California strong motion earthquake stations." *Rep. No. 62-55*, Dept. of Engrg., Univ. of California, Los Angeles, Calif.

Elsabee, F., and Morray, J. P. (1977). "Dynamic behavior of embedded foundations." *Rep. No. R77-33*, Dept. of Civ. Engrg., MIT, Cambridge, Mass.

Fenves, G. L., and DesRoches, R. (1994). "Response of the northwest connector in the Landers and Big Bear Earthquakes." *Rep. No. UCB/EERC-94/12*, Earthquake Engineering Research Center, Univ. of California, Berkeley, Calif.

Gohl, W. B. (1993). "Response of pile foundations to earthquake shaking — general aspects of behavior and design methodologies." *Proc., Seismic Soil/Struct. Interaction Seminar*, Vancouver.

Iguchi, M., and Luco, J. E. (1982). "Vibration of flexible plate on viscoelastic medium." *J. Engrg. Mech.*, ASCE, 108(6), 1103–1120.

Kausel, E. (1974). "Forced vibrations of circular foundations on layered media." *Rep. No. R74-11*, Dept. of Civ. Engrg., MIT, Cambridge, Mass.

Liou, G.-S., and Huang, P.-H. (1994). "Effect of flexibility on impedance functions for circular foundations." *J. Engrg. Mech.*, ASCE, 120(7), 1429–1446.

Ljung, L. (1987). *System identification: Theory for the user*. Prentice Hall, Englewood Cliffs, NJ.

Ljung, L. (1995). *System identification toolbox, users guide*. The Math Works, Inc., Natick, Mass.

Luco, J. E. (1980). "Linear soil-structure interaction." *Soil-structure interaction: The status of current analysis methods and research*, J. J. Johnson, ed., *Rep. No. NUREG/CR-1780 and UCRL-53011*, U.S. Nuclear Regulatory Commission, Washington, D.C. and Lawrence Livermore Laboratory, Livermore, Calif.

Novak, M. (1991). "Piles under dynamic loads." *Proc., 2nd Int. Conf. on Recent Advances in Geotech. Engrg. and Soil Dyn.*, Univ. of Miss.-Rolla, Rolla, Mo., 2433–2456.

Pandit, S. M. (1991). *Modal and spectrum analysis.* Wiley, New York.

Riggs, H. R., and Waas, G. (1985). "Influence of foundation flexibility on soil-structure interaction." *J. Earthquake Engrg. Struct. Dyn.*, 13(5), 597–615.

Rodriguez-Ordonez, J. A. (1994). "A new method for interpretation of surface wave measurements in soils," PhD dissertation, North Carolina State Univ., Raleigh, N.C.

Roesset, J. M. (1980). ''A review of soil-structure interaction.'' *Soil-structure interaction: The status of current analysis methods and research*, J. J. Johnson, ed., *Rep. No. NUREG/CR-1780 and UCRL-53011*, U.S. Nuclear Regulatory Commission, Washington, D.C. and Lawrence Livermore Laboratory, Washington, D.C.

Safak, E. (1991a). ''Identification of linear structures using discrete-time filters.'' *J. Struct. Engrg.*, ASCE, 117(10), 3064–3085.

Safak, E. (1991b). ''Adaptive modeling, identification, and control of dynamic structural systems. I: Theory.'' *J. Struct. Engrg.*, ASCE. 115(11), 2386–2405.

Schnabel, P. B., Lysmer, J., and Seed, H. B. (1972). ''SHAKE: A computer program for earthquake response analysis of horizontally layered soil deposits.'' *Rep. No. UCB/EERC-72/12*, Earthquake Engineering Research Center, Univ. of California.

Seed, R. B., Dickenson, S. E., and Mok, C. M. (1992). ''Recent lessons regarding seismic response analyses of soft and deep clay sites.'' *Proc., Seminar on Seismic Des. and retrofit of bridges*, Earthquake Engineering Research Center, Univ. of California, Berkeley, Calif., and Div. of Structures, California Dept. of Transportation, Sacramento, Calif., 18–39.

Seed, H. B., Romo, M. P., Sun, J. I., Jaime, A., and Lysmer, J. (1988). ''The Mexico Earthquake of September 19, 1985—relationships between soil conditions and earthquake ground motions.'' *Earthquake Spectra*, 4(4), 687–729.

Stewart, J. P., and Fenves, G. L. (1998). ''System identification for evaluating soil-structure interaction effects in buildings from strong motion recordings.'' *J. Earthquake Engrg. Struct. Dyn.*, 27, 869–885.

Stewart, J. P., Seed, R. B., and Fenves, G. L. (1999). ''Seismic soil-structure interaction in buildings. II: Empirical results.'' *J. Geotech. Engrg.*, ASCE, 125(1), 38–48.

Stewart, J. P., and Stewart, A. F. (1997). ''Analysis of soil-structure interaction effects on building response from earthquake strong motion recordings at 58 sites. *Rep. No. UCB/EERC-97/01*, Earthquake Engineering Research Center, Univ. of California, Berkeley, Calif., 742.

Todorovska, M. I. (1996). ''Second Preliminary Release Of Records Of The Northridge Earthquake (17 January, 1994) At Stations Of The Los Angeles Strong Motion Network,'' Univ. of Southern California, Los Angeles, Calif.

Uniform building code, 1997 edition. (1997). International Conference of Building Officials, Whittier, Calif.

Veletsos, A. S., and Meek, J. W. (1974). ''Dynamic behavior of building-foundation systems.'' *J. Earthquake Engrg. Struct. Dyn.*, 3(2), 121–138.

Veletsos, A. S., and Nair, V. V. (1975). ''Seismic interaction of structures on hysteretic foundations.'' *J. Struct. Engrg.*, ASCE, 101(1), 109–129.

Veletsos, A. S., and Verbic, B. (1973). ''Vibration of viscoelastic foundations.'' *J. Earthquake Engrg. Struct. Dyn.*, 2(1), 87–102.

Veletsos, A. S., and Wei, Y. T. (1971). ''Lateral and rocking vibrations of footings.'' *J. Soil Mech. and Found. Div.*, ASCE, 97(9), 1227–1248.

APPENDIX II.   NOTATION

The following symbols are used in this paper:

A_f = area of foundation;

a_0 = normalized frequency, $= \omega r / V_s$;

c = internal damping of single-degree-of-freedom structure;

c_u, c_θ = coefficients of foundation translational and rotational dashpots, respectively;

d = delay between $x(t)$ and $y(t)$, used in parametric system identification;

e = foundation embedment;

$f, \tilde{f}, \tilde{f}^*$ = fixed-, flexible-, and pseudoflexible-base fundamental mode frequencies, respectively;

G = shear modulus of soil;

H = total height of structure from base to roof;

h = effective height of structure (i.e., distance above foundation-level at which building's mass can be concentrated to yield same base moment that would occur in actual structure assuming linear first-mode shape);

I_f = moment of inertia of foundation;

i = $\sqrt{-1}$, also occasionally used as modal index;

J = number of modes used to model n-degree-of-freedom structure in system identification analysis ($J < n$);

$(K_u)_E$ = static translational stiffnesses for foundation on finite soil layer and foundation embedded into finite soil layer [Eq. (4)];

$(K_\theta)_E$ = static rotational stiffnesses for foundation on finite soil layer and foundation embedded into finite soil layer [Eq. (4)];

k = lateral stiffness of single-degree-of-freedom structure;

k_u, K_u = dynamic and static translational stiffnesses, respectively, for foundation on half-space;

$\bar{k}_u, \bar{k}_\theta$ = complex-valued dynamic foundation impedance for translation and rocking deformations, respectively;

k_θ, K_θ = dynamic and static rotational stiffnesses, respectively, for foundation on half-space;

m = generalized mass of structure for fundamental mode;

n = number of structural degrees-of-freedom;

r = radius of circular foundation;

r_u, r_θ = radii that match area and moment of inertia, respectively, of assumed circular foundation in impedance function formulations to actual foundation area and moment of inertia;

s = variable for Laplace-transformed functions, units of frequency;

$T, \tilde{T}, \tilde{T}^*$ = fixed-, flexible-, and pseudoflexible-base periods, respectively, for fundamental mode;

u = displacement of single-degree-of-freedom structure relative to its base;

u_f = horizontal displacement of foundation relative to free-field;

u_g = free-field ground displacement;

V_s = shear-wave velocity of soil;

α_u, β_u = dimensionless parameters expressing frequency-dependence of foundation translational stiffness and damping, respectively [Eq. (2)];

$\alpha_u^*, \alpha_\theta^*$ = products of α_u and α_θ, respectively, and static foundation impedance modifiers for depth effects [Eq. (4)];

$\alpha_\theta, \beta_\theta$ = dimensionless parameters expressing frequency-dependence of foundation rocking stiffness and damping, respectively [Eq. (2)];

β = soil hysteretic damping ratio;

γ = ratio of structure-to-soil mass [Eq. (8)];

$\zeta, \tilde{\zeta}, \tilde{\zeta}^*$ = fixed-, flexible-, and pseudoflexible-base damping ratios, respectively, for fundamental mode;

$\tilde{\zeta}_0$ = foundation damping factor, defined in Eq. (6);

θ = base rocking of foundation slab;

λ = forgetting factor for exponential window used in parametric system identification analyses by recursive prediction error method;

ν = soil Poisson ratio;

σ = ratio of soil-to-structure stiffness [Eq. (7)]; and

ω = angular frequency (rad/s).